Retraction Notice

The Editor-in-Chief and the publisher have retracted this article, which was submitted as part of a guest-edited special section. An investigation uncovered evidence of compromised peer review and determined the paper is not relevant to the special section. The Editor and publisher no longer have confidence in the results and conclusions of the article.

CG did not agree with the retraction. MPG either did not respond or could not be reached.

Design and development of SER-UNet model for glaucoma image analysis

C. Gobinath and M. P. Gopinath*

Vellore Institute of Technology, School of Computer Science and Engineering, Vellore, Tamil Nadu, India

Abstract. Glaucoma is a life-threatening disease that must be diagnosed early before it causes blindness. It is a dangerous disease and challenging for ophthalmologists. Retinal diseases can be detected at earlier stages with the help of analyzing fundus images of the retina and through the retinal vessel segmentation process. However, traditional fully convolutional neural network-based equivalents have major drawbacks in segmentation such as a bifurcation breakup in the vascular map and lessening pixel connectivity of vessels. To overcome this drawback, we present the squeeze excitation residual UNet (SER-UNet) model for vessel segmentation. The proposed model uses a new type of residual block called SER residual blocks for vessel segmentation. Initially, the fundus image is read and downsampled by converting the input image into vector values. Then, it conducts segmentation by adding attention mechanism and residual structure into convolution blocks to find vessel regions accurately and aggregate the tiny vessel characteristics. It helps segment the image of the glaucoma affected region in the retina. Together with a pixelwise cross-entropy loss function, it shows excellent performance on fundus image segmentation. The performance of the proposed method is assessed with an accuracy of 98.90% and 98.31%, respectively, using the DRIVE and STARE datasets, respectively. © *2022 SPIE and IS&T* [DOI: 10.1117/1.JEI.31.4.041215]

1 Introduction

Glaucoma is a chronic condition of cranial nerve damage. It is the second leading source of blindness. Glaucoma affects the peripheral visual field at an early stage. It affects the vision and marks in loss of visual acuity, which causes severe sight destruction and complete vision loss.[1,2] Intraocular pressure causes glaucoma of two types: open-angle and angle-closure. Some of the possible causes for glaucoma are high eye pressure, age above 50, hypertension, past injury in the eye, and family history of glaucoma. Retinal diseases such as diabetic retinopathy and glaucoma can be monitored by the tiny changes in the retinal vessels, optic disc, and optic cup.[3,4] Manual monitoring of blood vessels for millions of glaucoma-infected patients is a difficult process. Deep learning techniques are used to segment vascular density from fundus images. Constructing vessel structures with quality images at varying lighting conditions is done by morphological algorithms.[5,6] The development of autosegmentation algorithms has enabled measuring useful parameters of the vascular map. Variants of convolutional neural networks (CNNs) have been developed for medical image analysis. UNet is the only model specially designed to classify and localize the disease for medical images. There are variants of the UNet model with skip connections called cascaded UNets. With an increase in the number of convolutions, a complex network structure achieves a higher level of network depth. In the up- and downsampling phases of a cascaded model, residual blocks are used with normalization techniques.[7–9] Also, the individual skip connection preserves low-level pixel information by the transient of indices from the encoder to the decoder. Skip connections retain the edge

---

*Address all correspondence to M. P. Gopinath, mpgopinath@vit.ac.in

information and tiny vessel details lost during each convolution operation of the proposed model.[10] A residual connection-based network reduces the number of parameters by evolving the fully convolutional network (FCN) layer and dumping the downsampling part. The attention mechanism plays a vital role in vessel segmentation, which recalibrates features maps and integrates squeeze and excitation (SE) blocks into a fully connected neural network. Retinal vessel morphology is necessary for the surgical plan, diagnosis, and treatment based on the severity. It avoids vascular disorders and inability due to glaucoma and diabetes. To use spatial SE blocks that perform well as compared with channelwise SE blocks in segmentation performance, SE module variants are implemented: (i) spatial squeezing and channel excitation, (ii) channel squeezing and spatial excitation, and (iii) combined channel and spatial SE. SE blocks lead to minimum execution complexity of around 1.5%. The optimal position to place the SE block in Fully convolutional neural network is after encodes, decoders, bottleneck, and classifier. Finally, SE blocks yield a regular enhancement in segmentation performance.[11] Retinal images with pixel-level annotation have ground-truth at each pixel to train a deep neural network. Classifying the difference between thin and thick retinal vessels is difficult. The DCNN model identifies intervessel differences, but it ignores some thin-walled vessels of the retina during the downsampling process. Arteries are retrieved in the decoder by upsampling layers. The image patches are first converted into a retinal blood vessel map, which is segmented using a UNet encoder and decoder framework with network skip connections.[12]

This paper makes the following contributions:

- The innovative SER-UNet model combines an attention mechanism to aggregate spatial features and residual blocks to lessen vessel misclassification.
- The inclusion of intra- and interskip connections from residual block identifies multiscale features including tiny vessel structures.
- The efficiency of the proposed model is estimated in the public datasets, DRIVE and STARE.

2 Background

According to the WHO, in 2021, it was estimated that 12 million people are affected by glaucoma, and almost 1.2 million are blind as a result of the disease. The task of detecting the presence of glaucoma is very tedious due to the complex structure of vessels, optic cup shape, and the nature of glaucoma. Detecting glaucoma in the early stage is difficult for ophthalmologists. However, when glaucoma is detected in the early stage, it can be controlled with proper treatment. Detection can be carried out by visual field loss tests, manual assessment via an ophthalmoscope, and fundus images. Current diagnostic methods rely on traditional methods based on human experience. Recent advancements in image analysis have paved the way to analyzing fundus images. Image processing techniques are used to detect glaucoma by extracting the required information from the image.

3 Related Work

CNN models with attention residual UNet include segmentation and classification of retinal vessels.[13] The addition of attention based on residual units eases and improves the training process. To classify the preprocessed data, the attention-based ResUNet architecture is used. The fundus images are classified into glaucoma and nonglaucoma cases.[14] The classified fundus images are further reconstructed into their original form with the UNets upsampling process. The proposed method for image analysis is applied to the open-access DRIVE and STARE datasets. The performances of the proposed method is verified by the performance metrics, such as sensitivity (Se), specificity (Sp), accuracy (AC), $F1$-score (F1), and phi coefficient as the evaluation index. The performance of the hybrid network is achieved at varying network depths. SE is based on the deep learning method. It was developed to satisfy the main requirements such as feature aggregation and vessel segmentation.[15] This method initially resizes and preprocesses to a grayscale image. To extract growing arteries, maximum eigenvectors of the Hessian matrix are used for segmentation. There are two levels of classification. The first method employs SE and

the variant of the residual blocks in memory to perform robust feature extraction. Next, it uses a basic convolution layer architecture for classification. It categorizes glaucoma and nonglaucoma if both modules give the same result. The proposed method's performance is measured using precision, specificity, recall, and accuracy for the DIARETDB1 dataset images and hospital images.[16] The values and output are compared with existing methods.

The attention residual U network (AReN-UNet) model was designed for the detection of glaucoma, diabetic retinopathy, etc. It presents a cascaded AReN-UNet to get better convergence and solidity of the system.[17,18] A feature map of each convolution block is passed to subsequent UNet models. A network with aggregated residual structures will improve the representation abilities of a vascular map by reducing vessel breakdowns.[19] The proposed image analysis methods are tested on the open-access datasets DRIVE and CHASE DB1 as well as one hospital dataset. The proposed network achieves current performance in terms of accuracy, $F1$-score, sensitivity, specificity, and area under the curve. The UNet model with a strong training strategy uses data augmentation. The available labeled samples were used efficiently with data augmentation. The model specialty has a contracting path for classification and expanding path for localization of electron microscopy images.[20] Localization is the most needed part of all biomedical segmentation applications. It outperforms the CNN model in the International Symposium on Biomedical Imaging (ISBI) challenge for segmentation.[21] A simplified version of the visual imagery network is presented based on the ResUNet model.[22] In the contracting and expansion paths, it has batch normalization (BN) and residual blocks. The network depth has been reduced, as has the count of convolutions in each layer, which has been reduced from (64, 128, 256, 512, 1024) to (16, 16, 16, 16). The network is trained using patch inputs and a classification loss function that determines the division of every pixel toward the arterial hierarchy.[7,23]

The brightest spot algorithm is designed for the input image validation and region of interest detection using the LeCun network (LeNet) architecture. It is discussed under computer-aided diagnosis of fundus images for glaucoma detection. UNet is considered to be an efficient algorithm for medical image segmentation.[24,25] Optic disc segmentation is done by UNet, and vector values are forwarded to classifiers, such as SVM, neural network, and AdaBoost.[26–29] The effect of shorter and longer skip connections on a fully convolutional network has been discussed for modifying the depth of the network.[10,30,31]

Based on the literature review, it is observed that significant research in deep learning-based models focuses on the role of the residual network in retinal vessel segmentation. Gradient flow in shallow layers is achieved by long skip connections. Short skip connections on FCNs increase convergence speed and allow for training a deeper network, and it can achieve better accuracy on the fundus image dataset. U-Net misses some of the vessel details present in an image during segmentation. Using the variants of CNN models with attention mechanisms for image segmentation has extended its use into additional areas of research, so, we employ variants of the CNN model in our study to improve the accuracy (Table 1).

Table 1 Overview of deep learning-based methods for segmenting retinal blood artery.

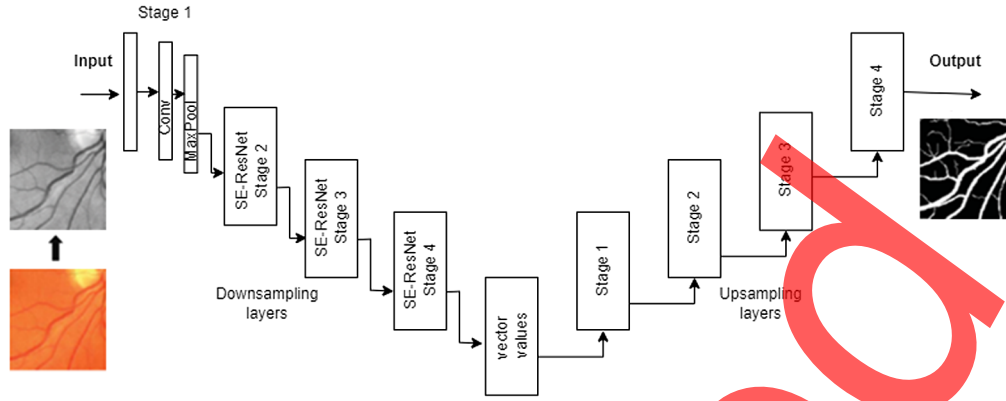| S.No.	Year/citation	Model/architecture
1	2021[14]	BSERU-Net (before activation SE residual UNet)
2	2021[16]	CNN
3	2021[19]	Attention ResU-Net
4	2021[7]	CNN
5	2021[26]	UNet
6	2020[10]	RCED-Net (residual conn-based encoder–decoder network)
7	2021[21]	Dense U-Net
8	2019[32]	Cascade refined U-Net
9	2019[33]	Trilogy of skip connection deep networks

Fig. 1 Flow of the proposed SER-UNet model.

4 Proposed Method

SER-UNet aims to combine attention and residual blocks to reduce vessel classification errors. It improves vessel pixel connectivity and reduces bifurcation breakup inside the vascular map. Thin vessels are captured by including cascaded network intra- and interskip connections. The proposed model's efficiency is approximated using the STARE and DRIVE datasets.

Figure 1 shows the network architecture. In total, it has 23 convolutional layers. It has a down-sampling part and an upsampling part. The downsampling part follows the architecture of the CNN model by doubling the number of characteristic channels at each block. It consists of two 3×3 convolutions that repeat twice and followed by a 2×2 max-pooling layer. For down-sampling, the stride value is set to 2. An expansive path halves the number of feature channels with cropping. The feature vector is constructed at the last stage by a 1×1 convolution operation for the corresponding classes shown. The residual path is the sum of the total number of residual transformations defined as

$$X(i) = \sum_{j=1}^{n} T_j(i), \tag{1}$$

where n denotes the attributes, T_j is a distinct residual path for each input, and output y after implementing the residual function as follows:

$$Y = \sum_{j=1}^{n} T_j(i) + i. \tag{2}$$

The convolutional block with the preactivation function processes the intermediate feature ($F \in R^{C*H*W}$) with one-dimensional channelwise attention plot ($A_c \in R^{C*1*1}$) and two-dimensional spatial maps as follows ($A_s \in R^{1*H*W}$).

Elementwise multiplication is used to represent the attention feature maps as

$$F' = A_c(F) \otimes F, F'' = A_s(F') \otimes F'. \tag{3}$$

Deeper networks have to be trained to perform complex functions. Degradation problems occur with an increase in depth of the network, i.e., performance degradation occurs. The use of a batch normalization network with a standardized input as well as regular weight initialization via normalization ensures that the gradients have good norms. All global features and contextual information are used by the convolutional encoder and decoder. It can complete the training work with a small number of samples. The influence of skip connections plays a major role in the residual learning process. Long skip connections allow gradients to flow in shallow layers. Short skip connections are fully connected networks enhancing the convergence speed and enabling deep network training without the vanishing gradient problem.[34,35]

Fig. 2 Representation of précised edge information from the input fundus image.

For complex skip connections, the semantic fundus image categorization procedure is described as a transport method from the normal image to the labeled segmentation target-domain corresponding to each pixel. We transform the image constantly in the contracting path and expansion path to reach the final stage. Spatial and semantic information is lost at each stage of transformation. To alleviate this problem, UNet follows the skip connection stage by stage.

In the proposed model, the encoder and decoder of the intranetwork contains skip connections to transfer feature maps with minimal information loss (Fig. 2). The main contribution of the network skip connection is the concatenation of the encoder and decoder convolved features to balance the information loss during the downsampling process. In the meantime, correcting errors in vessel maps is critical while identifying multiscale features. We use the network skip connections to send convolved features from the encoder to the decoder and concatenate them with the convolved features obtained by the following network. Multiclass features such as thin and thick vessels are distinguished from these types of skip connections.

4.1 *Attention Mechanism in the U-Shaped Network*

The SE block multiplies the output channels, and channelwise feature interactions are done.[36] Approximation of the low- and high-level attention maps is done for fundus images. These maps are fused in input fundus images to identify vessel regions. We use the spatial squeeze and channel excitation block with key feature map $X = [x_1, x_2, n, x_c]$ and channel combination $x_i \varepsilon R^{H \times W}$. At the average pooling layer, the spatial squeeze is performed, and the vector formed at the final element is $z \in R^{1 \times 1 \times C}$

$$Z_k = \frac{1}{H * W} \sum_{i}^{H} \sum_{j}^{H} X_k(i, j). \tag{4}$$

The activations z with the interval (0, 1) pass to a sigmoid layer $\sigma(z)$. Feature map X is recalibrated from the resultant vector represented as

$$X = [\sigma(Z_1)x_1, \sigma(Z_2)x_2, \ldots, \sigma(Z_c)x_c. \tag{5}$$

SE structures can be used in frameworks such as VGGNets, ResNets, and InceptionNets. Inside a block, we integrate spatial features and channelwise SE. To improve performance, we incorporate an attention mechanism into the residual blocks. SE structures strive to continuously improve the generalization ability of vessels.

The attention mechanism can aggregate spatial features that contain relevant information while ignoring those that do not. Five-step SE blocks are introduced into residual blocks. It has a computational complexity of <1%. It embeds global information from each channel with dimensions $H \times W \times C$, as shown in Fig. 3. Adaptive reconstruction is done by assigning weights to each channel. In segmentation, the pixelwise cross-entropy loss function is used to analyze artery and nonartery pixels. In terms of ACC, Sp, and Se, we found that the
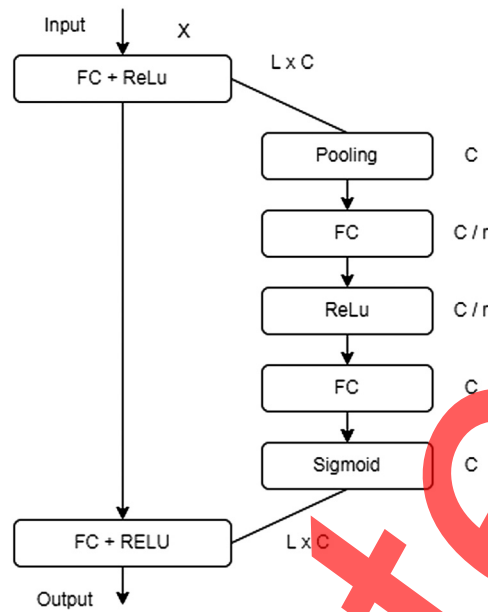
Fig. 3 Attention mechanism.

cross-entropy function outperforms the dice loss function, so this advancement is consistent, which is more beneficial inside the artery segmentation. CE loss function is represented as

$$\text{CE} = -\frac{1}{P}\sum_{i=1}^{n} t_i \ln(x_i) + (1 - t_i)\ln(1 - t_i), \tag{6}$$

where x_i likelihood of the input pixel and P is the number of pixels. The vessel pixel value is zero or one represented as true label i and t_i, respectively.

5 Result and Discussion

5.1 Image Dataset

The proposed system is evaluated using the DRIVE database with 40 fundus images and the STARE database that have 20 retinal fundus images. For classification, DRIVE uses 20 glaucoma and 20 normal images with a 565×584 pixel resolution.[14] STARE uses 10 glaucoma and 10 normal images with a 700×605 pixel resolution. These images are taken from fundus camera works on the concept of monocular indirect ophthalmoscopy. To segment blood vessels precisely, we convert red green blue (RGB) to gray-scale and normalize those images. Blood vessels are enhanced by applying histogram equalization, which increases the contrast of the image. The patch size is set to 48×48 for datasets.

5.2 Data Augmentation Process

The size of the dataset can be augmented further, and the overfitting problem can be reduced by undergoing a procedure called data augmentation. By applying the data augmentation technique, the number of training images is increased four times.[37,38] For the DRIVE and STARE datasets, 240,000 and 180,000 patches, respectively, are retrieved and then used.

5.3 Experimental Analysis

The proposed SER-UNet model is tested using a PC equipped with a GPU Nvidia GTX1080, an i7-10th generation processor, 16 GB RAM, and 64-bit system software. TensorFlow and Keras
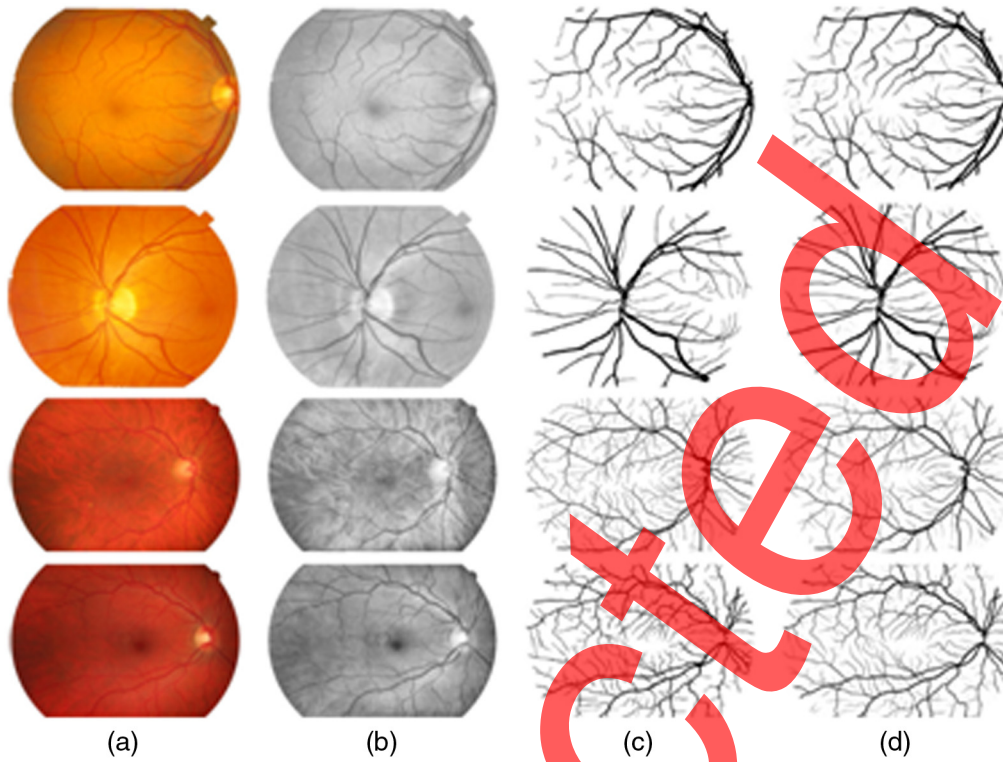
Fig. 4 (a) RGB fundus images, (b) grayscale conversion, (c) ground-truth image, and (d) segmented fundus image obtained from the SER-UNet model.

packages in Python programming are the software specifications used. Figure 4(a) describes the dataset of fundus images with varying illumination, Fig. 4(b) shows the grayscale conversion of fundus images, Fig. 4(c) shows the ground-truth of dataset, and Fig. 4(d) shows the concise segmentation result efficiency of the suggested SER-UNet method. Rows 1 and 2 contain results from the DRIVE dataset. Rows 3 and 4 contain results from the STARE dataset.

5.4 *Evaluation Metrics*

Four metrics were used to show the value and accuracy of the anticipated segmentation technique in Table 2. The metrics are $F1$-score, sensitivity, specificity, and accuracy.

To quantify these metrics, the following parameters must be estimated:

$$\text{Accuracy} = \frac{(\text{TP} + \text{TN})}{\text{TP} + \text{FP} + \text{TN} + \text{FN}}, \tag{7}$$

$$\text{Sensitivity} = \frac{\text{Number of True Positive}}{\text{Number of True Positive} + \text{Number of False Negative}}, \tag{8}$$

$$\text{Specificity} = \frac{\text{Number of True Negative}}{\text{Number of True Negative} + \text{Number of False Positives}}, \tag{9}$$

$$F1\text{-score} = 2 \times \left(\frac{\text{precision} \times \text{recall}}{\text{precision} + \text{recall}} \right). \tag{10}$$

The $F1$-score, accuracy, sensitivity, and specificity of the system are given in Fig. 5; these relate to the classification performance of the SER-UNet model.

Table 2 Ablation analysis of the proposed model.

| Methodology proposed by	Classifier	Dataset	Specificity (%)	Sensitivity (%)	Accuracy (%)	F1-score (%)
Li and Rahardja et al.[14]	BSERU-Net (before activation SE residual UNet)	DRIVE	97.00	78.00	96.20	83.24
Das et al.[16]	CNN	DIARETDB	97.60	—	98.70	—
Rahman et al.[19]	Attention ResU-Net	CHASE_DB1	85.60	82.01	97.70	82.34
Gegundez-Arias et al.[7]	CNN	STARE	97.64	84.41	95.09	—
Shinde et al.[26]	UNet	RIM-ONE	95.11	—	97.90	91.00
Khan et al.[10]	RCED-Net (residual conn-based encoder–decoder network)	CHASE_DB1	98.10	84.40	97.22	—
Zhao et al.[21]	Dense U-Net	STARE	97.00	85.11	97.94	—
Zhang et al.[32]	Cascade refined U-Net	DRIVE	98.77	73.64	93.97	77.69
Hua et al.[33]	Trilogy of skip connection deep networks	PRIVATE	82.10	83.50	90.60	—
Proposed methodology	SER-UNet	STARE	97.60	83.23	98.31	79.27
Proposed methodology	SER-UNet	DRIVE	98.89	85.54	98.90	84.62
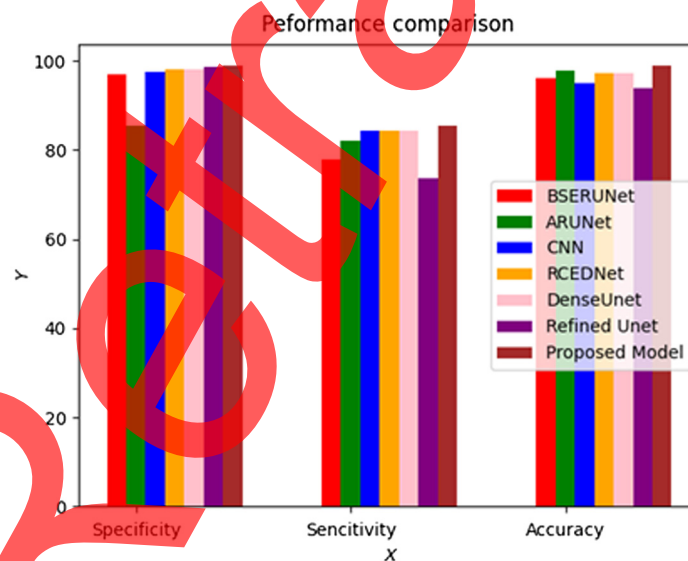
Fig. 5 Performance comparison of the proposed model with existing classifiers.

Table 3 compares specificity as well as accuracy for every fold, along with their average value. The value obtained from each fold is found closer to the average value, so there is not much variation in the performance.

The observed graph values from Fig. 6 state that for 10 epochs, the error rate is predicted. The error rate can be decreased by increasing the epoch count. At the 10th epoch, the predicted err_rate is 0.35, training_loss is 1.77, and validation_loss is 1.03, as listed in Table 4.

Table 3 Evaluation of sensitivity, specificity, and accuracy for every fold.

Testing fold	Specificity	Accuracy
First fold	98.72	99.32
Second fold	99.14	98.35
Third fold	98.95	99.05
Fourth fold	98.46	99.04
Fifth fold	99.21	98.76
Average	98.89	98.90
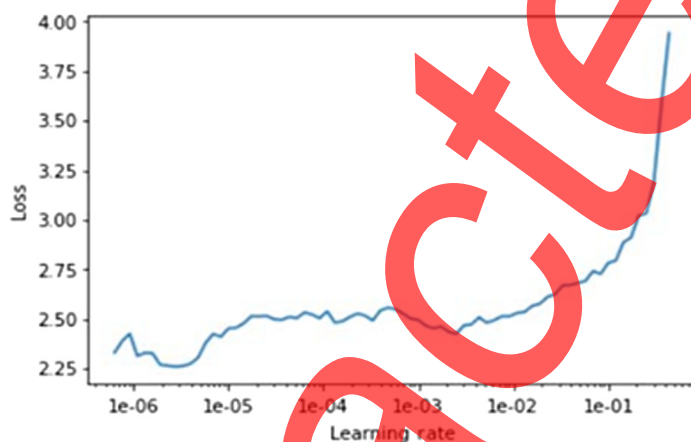
Fig. 6 SER-UNet learning error rate.

Table 4 SER-UNet error rate with respect to time.

No of epochs	Err_rate	Training_loss	Validation_loss	Time elapsed
0	0.560457	2.97845	1.910259	00:50
1	0.487741	2.25656	1.454955	00:49
2	0.413595	2.32246	1.278932	00:49
3	0.454988	2.40042	1.413178	00:48
4	0.404645	2.25984	1.431500	00:48
5	0.356498	2.35645	1.305598	00:47
6	0.324986	1.92231	1.236451	00:45
7	0.354456	1.80144	1.256846	00:46
8	0.354989	1.68790	1.198422	00:45
9	0.359788	1.77901	1.036540	00:47

6 Conclusion

This article proposed a deep learning architecture with a deep cascading mechanism called SER-UNet, which used an SE residual block in the ResUNet model for blood vessel segmentation. The incorporation of the proposed network with accumulated residual blocks and attention

techniques improved the performance by enhancing vessel generalization and interpretation qualities. It showed a better enrichment of images than other existing methods. Then, the proposed proficient segmentation model helped the user to classify the visual difference in segmenting the infected regions. Metrics, such as sensitivity, specificity, and accuracy, were used to assess the effectiveness of the proposed model, which achieved 98.90% accuracy, which is better than other existing methods.

References

1. E. O. Rodrigues, A. Conci, and P. Liatsis, "ELEMENT: multi-modal retinal vessel segmentation based on a coupled region growing and machine learning approach," *IEEE J. Biomed. Health Inf.* **24**(12), 3507–3519 (2020).
2. M. Alhussein, K. Aurangzeb, and S. I. Haider, "An unsupervised retinal vessel segmentation using Hessian and intensity based approach," *IEEE Access* **8**, 165056–165070 (2020).
3. M. Soorya, A. Issac, and M. K. Dutta, "An automated and robust image processing algorithm for glaucoma diagnosis from fundus images using novel blood vessel tracking and bend point detection," *Int. J. Med. Inf.* **110**, 52–70 (2018).
4. Z. Fan et al., "A hierarchical image matting model for blood vessel segmentation in fundus images," *IEEE Trans. Image Process.* **28**(5), 2367–2377 (2018).
5. T. Saba et al., "Fundus image classification methods for the detection of glaucoma: a review," *Microsc. Res. Tech.* **81**(10), 1105–1121 (2018).
6. K. Yu et al., "Deep-learning-empowered breast cancer auxiliary diagnosis for 5GB remote E-health," *IEEE Wireless Commun.* **28**(3), 54–61 (2021).
7. M. E. Gegundez-Arias et al., "A new deep learning method for blood vessel segmentation in retinal images based on convolutional kernels and modified U-Net model," *Comput. Methods Prog. Biomed.* **205**, 106081 (2021).
8. K. Yu et al., "Securing critical infrastructures: deep-learning-based threat detection in IIoT," *IEEE Commun. Mag.* **59**(10), 76–82 (2021).
9. K. Yu et al., "Secure artificial intelligence of things for implicit group recommendations," *IEEE Internet Things J.* **9**(4), 2698–2707 (2021).
10. T. M. Khan et al., "Residual connection-based encoder decoder network (RCED-Net) for retinal vessel segmentation," *IEEE Access* **8**, 131257–131272 (2020).
11. A. G. Roy, N. Navab, and C. Wachinger, "Recalibrating fully convolutional networks with spatial and channel "squeeze and excitation" blocks," *IEEE Trans. Med. Imaging* **38**(2), 540–549 (2018).
12. Y. Wu et al., "NFN+: a novel network followed network for retinal vessel segmentation," *Neural Networks* **126**, 153–162 (2020).
13. S. Gayathri, V. P. Gopi, and P. Palanisamy, "A lightweight CNN for diabetic retinopathy classification from fundus images," *Biomed. Signal Process. Control* **62**, 102115 (2020).
14. D. Li and S. Rahardja. "BSEResU-Net: an attention-based before-activation residual U-Net for retinal vessel segmentation," *Comput. Methods Prog. Biomed.* **205**, 106070 (2021).
15. L. Gong et al., "Automated pulmonary nodule detection in CT images using 3D deep squeeze-and-excitation networks," *Int. J. Comput. Assist. Radiol. Surg.* **14**(11), 1969–1979 (2019).
16. S. Das et al., "Deep learning architecture based on segmented fundus image features for classification of diabetic retinopathy," *Biomed. Signal Process. Control* **68**, 102600 (2021).
17. Y. Lv et al., "Attention guided U-net with atrous convolution for accurate retinal vessels segmentation," *IEEE Access* **8**, 32826–32839 (2020).
18. I. Atli and O. S. Gedik, "Sine-net: a fully convolutional deep learning architecture for retinal blood vessel segmentation," *Eng. Sci. Technol. Int. J.* **24**(2), 271–283 (2021).
19. A. A. Rahman et al. "Robust segmentation of vascular network using deeply cascaded AReN-UNet," *Biomed. Signal Process. Control* **69**, 102953 (2021).
20. V. Malathi and M. P. Gopinath, "Classification of pest detection in paddy crop based on transfer learning approach," *Acta Agric. Scand., Sect. B—Soil Plant Sci.* **71**, 1–8 (2021).
21. R. Zhao et al., "A nested U-shape network with multi-scale upsample attention for robust retinal vascular segmentation," *Pattern Recognit.* **120**, 107998 (2021).

22. Y. Tang et al., "ResWnet for retinal small vessel segmentation," *IEEE Access* **8**, 198265–198274 (2020).
23. K. He et al., "Deep residual learning for image recognition," in *Proc. IEEE Conf. Comput. Vision and Pattern Recognit.* (2016).
24. P. M. Samuel and T. Veeramalai, "VSSC Net: vessel specific skip chain convolutional network for blood vessel segmentation," *Comput. Methods Prog. Biomed.* **198**, 105769 (2021).
25. V. Sathananthavathi and G. Indumathi, "Encoder enhanced atrous (EEA) UNet architecture for retinal blood vessel segmentation," *Cognit. Syst. Res.* **67**, 84–95 (2021).
26. R. Shinde, "Glaucoma detection in retinal fundus images using U-Net and supervised machine learning algorithms," *Intell.-Based Med.* **5**, 100038 (2021).
27. G. Huang et al., "Densely connected convolutional networks," in *Proc. IEEE Conf. Comput. Vision and Pattern Recognit.* (2017).
28. O. Ronneberger, P. Fischer, and T. Brox, "U-net: convolutional networks for biomedical image segmentation," *Lect. Notes Comput. Sci.* **9351**, 234–241 (2015).
29. S. Feng et al., "CcNet: a cross-connected convolutional network for segmenting retinal vessels using multi-scale features," *Neurocomputing* **392**, 268–276 (2020).
30. L. Tan et al. "Secure and resilient artificial intelligence of things: a HoneyNet approach for threat detection and situational awareness," *IEEE Consum. Electron. Mag.* **11**(3), 69–78 (2021).
31. P. Khojasteh et al., "Exudate detection in fundus images using deeply-learnable features." *Comput. Biol. Med.* **104**, 62–69 (2019).
32. S. Zhang et al., "Simultaneous arteriole and venule segmentation of dual-modal fundus images using a multi-task cascade network," *IEEE Access* **7**, 57561–57573 (2019).
33. C.-H. Hua et al., "Bimodal learning via trilogy of skip-connection deep networks for diabetic retinopathy risk progression identification," *Int. J. Med. Inf.* **132**, 103926 (2019).
34. C. Wang et al., "Dense U-net based on patch-based learning for retinal vessel segmentation," *Entropy* **21**(2), 168 (2019).
35. G. García et al., "Circumpapillary OCT-focused hybrid learning for glaucoma grading using tailored prototypical neural networks," *Artif. Intell. Med.* **118**, 102132 (2021).
36. G. García, A. Colomer, and V. Naranjo, "Glaucoma detection from raw SD-OCT volumes: a novel approach focused on spatial dependencies," *Comput. Methods Prog. Biomed.* **200**, 105855 (2021).
37. R. Asaoka et al., "Validation of a deep learning model to screen for glaucoma using images from different fundus cameras and data augmentation," *Ophthalmol. Glaucoma* **2**(4), 224–231 (2019).
38. W. M. Liao et al., "Clinical interpretable deep learning model for glaucoma diagnosis," *IEEE J. Biomed. Health Inf.* **24**(5), 1405–1412 (2019).

C. Gobinath is a research scholar in the School of Computer Science at Vellore Institute of Technology, Vellore, India. He received his MTech degree from SRM University, Kattankulathur, Chennai. His research interests focus on computer vision and image analysis and computer networks.

M. P. Gopinath is currently working as an associate professor in the School of Computer Science and Engineering, Vellore Institute of Technology, Vellore, India. He received his ME degree from SSN College of Engineering, Anna University, Chennai, and his PhD from VIT Vellore, India. He has 22+ journal publications. His research interests include image processing, machine learning, and algorithm analysis.